Published in final edited form as:
Dev Cell. 2015 January 26; 32(2): 231–240. doi:10.1016/j.devcel.2014.11.014.

Casein Kinase 1 Promotes Initiation of Clathrin-Mediated Endocytosis

Yutian Peng[1], **Alexandre Grassart**[1], **Rebecca Lu**[1], **Catherine C. L. Wong**[2], **John Yates III**[2], **Georjana Barnes**[1], and **David G. Drubin**[1,*]

[1]Department of Molecular and Cell Biology, University of California, Berkeley, Berkeley, CA 94720, United States

[2]Department of Chemical Physiology, The Scripps Research Institute, La Jolla, CA 92037, United States

Summary

In budding yeast, over 60 proteins functioning in at least 5 modules are recruited to endocytic sites with predictable order and timing. However, how sites of clathrin-mediated endocytosis are initiated and stabilized is not well understood. Here, the casein kinase 1 (CK1) Hrr25 is shown to be an endocytic protein and to be among the earliest proteins to appear at endocytic sites. Hrr25 absence or overexpression decreases or increases the rate of endocytic site initiation, respectively. Ede1, an early endocytic Eps15-like protein important for endocytic initiation, is an Hrr25 target and is required for Hrr25 recruitment to endocytic sites. Hrr25 phosphorylation of Ede1 is required for Hrr25-Ede1 interaction and promotes efficient initiation of endocytic sites. These observations indicate that Hrr25 kinase and Ede1 cooperate to initiate and stabilize endocytic sites. Analysis of the mammalian homologs CK1δ/ε suggests a conserved role for these protein kinases in endocytic site initiation and stabilization.

Introduction

Clathrin-mediated endocytosis (CME) plays critical roles in a cell's response to its environment by controlling plasma membrane protein and lipid composition and by mediating nutrient uptake. In budding yeast, over 60 proteins have been shown to appear and disappear at endocytic sites in a highly orchestrated manner (Kaksonen et al., 2005), suggesting that CME is a highly regulated process. Similarly, in mammalian cells over 40 proteins are recruited to sites of CME in a regular sequence (Taylor et al., 2011).

Although the later stages of CME are well described in budding yeast and mammalian cells, the processes by which CME sites are initiated and stabilized are still being worked out. Recent studies suggested a role for the adaptor protein AP2 and for FCHo1/2 in initiating

*Corresponding author: David Drubin, drubin@berkeley.edu, Phone: 510.642.3692, Fax: 510.643.0062.

and/or stabilizing early endocytic structures (Henne et al., 2010; Umasankar et al., 2012). In budding yeast AP2 and the FCHo1/2 homologue Syp1 are among the first proteins to arrive at endocytic sites (Carroll et al., 2011), but neither is important for initiation of CME. However, the Syp1-binding protein Ede1 plays a critical role in early endocytic events (Carroll et al., 2011). Ede1 is a yeast homologue of mammalian Eps15, which binds to FCHo1 (Reider et al., 2009) and the FCHo1/2-like protein SGIP1-α (Uezu et al., 2007). Ede1 is a highly phosphorylated protein (Sadowski et al., 2013; Stark et al., 2010). However, the role of Ede1 phosphorylation and the identity of the biologically relevant kinase(s) remain to be determined.

Proteomics studies implicated the protein kinase Hrr25, a member of a highly conserved CK1 subfamily, in physical interactions with several endocytic proteins including Ede1 (Breitkreutz et al., 2010; Ho et al., 2002), clathrin light chain (Ptacek et al., 2005), and Abp1 (Ho et al., 2002). Since many yeast endocytic proteins are phosphorylated (PhosphoGRID, www.phosphogrid.org), finding that a CK1 family member is present at endocytic sites could potentially provide new insights into endocytic regulation.

Among the six human CK1 family members, CK1δ and CK1ε are the most similar to Hrr25 based on sequence similarity (Petronczki et al., 2006), and both isoforms rescue the growth defects of an *hrr25* null mutant (Fish et al., 1995). A previous genome-wide RNA interference screen suggested a role of CK1δ in CME (Collinet et al., 2010). However, how CK1δ affects CME remained unexplored.

Results

Yeast CK1 Hrr25 is an early endocytic protein

To test whether Hrr25 plays a role in CME, we first determined whether this protein appears at endocytic sites in living yeast cells. Hrr25-3GFP expressed from the native *HRR25* genomic locus had no observable growth defects (Fig. S1A). This protein was detected at spindle pole bodies (SPBs, yeast centrosomes) and the bud neck, consistent with previous reports (Kafadar et al., 2003; Lusk et al., 2007), and at cortical spots similar to those observed for GFP-tagged endocytic proteins (Fig. 1A). Simultaneous two-color imaging of Hrr25-3GFP and Sla1-mCherry, an endocytic coat protein, demonstrated that Hrr25 is present at endocytic sites and arrives early relative to Sla1 (Fig. 1B). Moreover, Hrr25 appears at the plasma membrane for variable times, but in contrast to coat proteins, does not move into the cell (Fig. 1C). This behavior is a hallmark of the early endocytic proteins Ede1 and Syp1 (Stimpson et al., 2009), which are closely related to mammalian early endocytic proteins Eps15 (Gagny et al., 2000) and FCHo1/2 (Reider et al., 2009; Stimpson et al., 2009), respectively. We therefore compared Hrr25-3GFP and Ede1-GFP lifetimes on the plasma membrane. Average lifetimes of Hrr25-3GFP patches are shorter than those of Ede1-GFP (36.5 *vs* 52.7 s, Fig. 1D). Like Ede1-GFP, lifetimes of Hrr25-3GFP are highly variable, ranging from less than 30 seconds to greater than 2 minutes (Fig. 1E). Consistent with arrival at the earliest stages of CME, Hrr25 showed a high frequency of colocalization with Ede1 (66%), similar to Ede1's binding partner Syp1 (74%) (Fig. 1F, G). We further compared arrival times of Hrr25 to those of Ede1. Under our imaging conditions, we

observed that either Hrr25 or Ede1can appear on plasma membrane first, with the two proteins appearing to arrive simultaneously 20% of the time (Fig. 1H).

Loss of Hrr25 or its kinase activity results in initiation of fewer endocytic sites

To test whether Hrr25 functions in endocytosis, we first monitored endocytic uptake of the lipophilic dye FM4-64 in various *hrr25* mutant backgrounds. Relative to wild-type cells (73.4% FM4-64 uptake), *sla2*Δ (17.6%) and *ede1*Δ (68.6%) mutants had severe and mild uptake defects, respectively, while an *hrr25* null mutant had intermediate defects (31.6%) (Fig. 2A, B). The kinase-dead mutant (*hrr25(K38A)*), despite being integrated at the native genomic locus, expressed its protein product at higher levels compared to the isogenic wild-type *HRR25* (Fig. 2C), suggesting that Hrr25 phosphorylation promotes its turnover. However, like the *hrr25* null mutant, *hrr25(K38A)* failed to internalize FM4-64 efficiently (36.3% uptake compared to 70.3% for the wild-type strain) (Fig. 2A, B). Next we monitored kinetics of the endocytic machinery. Simultaneous imaging of Sla1-GFP, marking the endocytic coat module, and Abp1-RFP, marking the actin module, revealed that endocytic protein lifetimes in the *hrr25* null mutant were slightly increased (24.6 *vs* 21.4 s for Sla1-GFP lifetimes; 17.3 *vs* 11.5 s for Abp1-RFP lifetimes), but were not altered much in the kinase-dead mutant (21.1 *vs* 20.8 s for Sla1-GFP lifetimes; 12.0 *vs* 11.9 s for Abp1-RFP lifetimes). Additionally, both the Sla1 and Abp1 lifetimes became more variable in the *hrr25* mutants (Fig. 2D, E). Since the relatively small changes in endocytic kinetics seemed unlikely to account for the greatly reduced FM4-64 uptake in *hrr25* mutants, we next examined the number of endocytic sites formed. As shown in Figures 2F and G, both *hrr25* null and kinase-dead mutants showed a pronounced reduction in the number of endocytic sites present on surfaces of yeast cells. Approximately 4.2 Sla1-GFP patches are found on 10 μm^2 of the wild-type yeast cell surface at a given time. Loss of Hrr25 lowered the Sla1-GFP density to 57% of the wild-type density. Loss of Hrr25 kinase activity caused a similar decrease in Sla1-GFP density.

Hrr25 and Ede1 act synergistically in endocytic site initiation

Hrr25 is composed of a highly conserved kinase domain at its amino-terminus, a central domain, and a carboxyl-terminal proline/glutamine (P/Q)-rich domain (Fig. S1B). To test for the functions of the non-kinase regions of Hrr25, the P/Q-rich and the central domain were deleted and the resulting mutants tested for phenotypes. Compared to wild-type cells, mutants lacking the Hrr25 P/Q-rich domain (*hrr25*Δ*PQ*) showed slight defects in FM4-64 internalization, Sla1-GFP lifetime, and endocytic site initiation, whereas mutants lacking both the central and P/Q-rich domains (*hrr25*Δ*CT*) showed pronounced defects (Fig. S1C–G). These defects may be due to the fact that *hrr25*Δ*CT* has reduced protein levels (Fig. S1B). Interestingly, although *hrr25*Δ*PQ* exhibits only subtle defects, we observed a synthetic genetic effect when we combined *hrr25*Δ*PQ* with an *ede1* null allele. Neither of the single mutants exhibits detectable growth defects at various temperatures. However, the double mutant (*hrr25*Δ*PQ ede1*Δ) shows slow or no growth at 37 or 39°C (Fig. S1H). This genetic interaction prompted us to examine further the functional relationship between Hrr25 and Ede1. In a null mutant of the early endocytic protein Ede1, Sla1 and Abp1 were reported to have shorter lifetimes and a decrease in Sla1 patch density on the cell surface (Kaksonen et al., 2005; Stimpson et al., 2009). Combining various *hrr25* mutants with an

ede1 null allele did not greatly exacerbate Sla1 and Abp1 lifetime defects (Fig. 2D, E). However, the double mutants showed a dramatic synergy in loss of endocytic sites (Fig. 2F, G). The *hrr25*Δ and *ede1*Δ single mutants have patch densities that are 56% and 76% of the wild-type patch density, respectively, whereas the *hrr25*Δ *ede1*Δ double mutant exhibits a patch density that is 23% of the wild-type density. The above results are consistent with a role for Hrr25 in promoting endocytic site initiation and/or stabilizing endocytic sites.

Hrr25 overexpression increases the number of endocytic sites

We next set out to test whether overexpression of Hrr25 affects initiation of endocytic sites. We utilized a previously developed system to overexpress Hrr25 without changes in nutrients or temperature (McIsaac et al., 2011). Transcription of a *GAL* promoter-driven Hrr25-Myc was activated upon addition of nanomolar β-estradiol. Hrr25 levels showed an approximately 8-fold increase 4 hours after β-estradiol addition (Fig. 2H). The elevated Hrr25 levels had little effect on Sla1-GFP or Abp1-RFP lifetimes (Fig. 2I) but increased the number of endocytic sites by approximately 31% (Fig. 2J).

Hrr25 phosphorylates multiple endocytic proteins

To better understand how Hrr25 regulates the endocytic machinery, we purified wild-type and kinase-dead Hrr25 from yeast and tested their ability to phosphorylate 16 purified endocytic proteins or protein complexes. Similar to what was previously described for Hrr25 wild-type and kinase-dead mutant purified from *E. coli* (Corbett and Harrison, 2012), we observed that wild-type kinase migrated more slowly than the kinase-dead mutant on SDS-PAGE, likely due to auto-phosphorylation (Fig. S2A). Hrr25 purified from yeast readily phosphorylated casein, slightly phosphorylated histone H3, but did not phosphorylate histone H1 (Fig. S2B). We found that Hrr25 phosphorylated itself, Ede1, Syp1, Sla2, Las17, Bbc1, and Aim21, representing three different endocytic modules (Fig. S2C, D). Because of Hrr25's Ede1-dependent early arrival at endocytic sites and the similar phenotypes of *hrr25* and *ede1* mutants, we decided to focus our current studies on Ede1 phosphorylation.

Ede1 recruits Hrr25 to endocytic sites

Our previous studies established that Ede1 plays a crucial role in the recruitment and/or stabilization of several other early endocytic proteins (Carroll et al., 2011). We found that Hrr25 recruitment to endocytic sites completely depends on Ede1 (Fig. 3A). Importantly, Ede1 absence did not affect Hrr25 protein levels (Fig. S3A). Ede1 is a modular protein that is composed of, from the amino- to the carboxyl-terminus, three Eps15 homology (EH) domains, a proline-rich region (PP), a coiled-coil domain (CC) and a ubiquitin-associated domain (UBA) (Aguilar et al., 2003). Using deletion analysis we identified the Ede1 carboxyl-terminal region between the CC domain and UBA domain as being necessary for Hrr25 recruitment (Fig 3B and Fig. S3B). The same region was previously shown to be essential for Ede1's interaction with Syp1 (Reider et al., 2009). Consistent with the previously reported physical association between Ede1 and Hrr25 (Breitkreutz et al., 2010; Ho et al., 2002) and their similar dynamics at endocytic sites, we found that Hrr25 could pull down Ede1 from whole cell extracts (Fig. 3C).

Hrr25 phosphorylation of Ede1 is required for efficient initiation/stabilization of endocytic sites

To better understand how Hrr25 kinase activity affects Ede1 function, we first determined whether loss of kinase activity affects Hrr25 localization. We tagged Hrr25 kinase-dead mutant with three GFPs. Similar to the untagged kinase-dead Hrr25, Hrr25(K38A)-3GFP was expressed at elevated protein levels (Fig. S3D). Interestingly, the Hrr25 kinase-dead mutant did not localize at spindle pole bodies or at endocytic sites, and had a diffuse distribution throughout the cell (Fig. S3C). Furthermore, we directly compared Ede1-GFP by fluorescence microscopy in wild-type and kinase-dead mutant cells and found that loss of Hrr25 kinase activity resulted in ~50% reduction of Ede1 from endocytic sites (Fig. S3E, F). These results support a model in which Hrr25 catalytic activity is required for its own recruitment and for robust Ede1 recruitment to endocytic sites.

Ede1 is a highly phosphorylated protein. A total of 71 *in vivo* phosphorylation sites have been identified on Ede1 to date (PhosphoGRID). Our kinase assays established that Hrr25 phosphorylates Ede1 *in vitro* (Fig. S2C). We asked whether Hrr25 phosphorylates Ede1 *in vivo*. Because changes in gel mobility are hard to detect on large proteins like Ede1 (~151 kDa), we used a truncated mutant Ede1ΔPPCC, in which Ede1's proline-rich region and coiled-coil domain were deleted. Ede1ΔPPCC migrates as a doublet on SDS-PAGE. Upon treatment of alkaline phosphatase, the slower migrating band of Ede1ΔPPCC collapsed into the faster migrating band (Fig. 3D), indicating that the slower migrating band is a phosphorylated form of Ede1ΔPPCC. We found that loss of Hrr25 kinase activity results a similar but somewhat less complete migration change (Fig. 3D), providing evidence that Hrr25 phosphorylates Ede1 *in vivo*. The lack of a complete collapse of Ede1ΔPPCC into the faster migrating band suggests that Ede1 is likely to be phosphorylated by kinases in addition to Hrr25 *in vivo*. Indeed, Ede1 has previously been reported to be phosphorylated by Ark1 and Prk1 (Mok et al., 2010), two endocytic protein kinases that regulate organization and function of endocytic actin patches (Cope et al., 1999; Zeng and Cai, 1999).

Because Hrr25 phosphorylates multiple endocytic proteins, to understand how Hrr25 specifically affects Ede1 function, we set out to map Hrr25 phosphorylation sites on Ede1. We expressed and purified three Ede1 fragments (1–400, 375–918, 900–1381aa) from bacteria and subjected them to Hrr25 phosphorylation (Fig. 3E). Interestingly, Hrr25 only phosphorylated the carboxyl-terminal region between residues 900 and 1381, the same region of Ede1 important for Hrr25 recruitment to endocytic sites. The Ede1 carboxyl-terminus contains 40 phosphorylated residues according to PhosphoGRID, among which we identified 22 by mass spectrometry as being phosphorylated by Hrr25 *in vitro* (Fig. S3G). Mutation of these 22 overlapping phosphorylation sites had no obvious effect on Ede1 protein levels or lifetime on the plasma membrane (Fig. 3F, G). In contrast, Ede1(22A) and Ede1(22D) failed to recruit Hrr25 to endocytic sites (Fig. 3H), indicating that these phosphorylation sites are critical Ede1-Hrr25 interaction. We further examined how endocytosis was affected in these *ede1* phospho-mutants. Compared to wild-type *EDE1* cells, *ede1(22A)* and *ede1(22D)* cells exhibited similar Sla1 lifetimes (Fig. 3I). However, Sla1 patch density on the cell surface was reduced by 25% in *ede1(22A)* cells and by 15% in

ede1(22D) cells. *ede1(22D)* does not mimic the wild-type, possibly because aspartate does not always mimic phosphate groups faithfully (Dephoure et al., 2013), and likely because dynamic phosphorylation and dephosphorylation may be important for normal function. Taken together, the above results provide evidence that Hrr25 phosphorylation of the Ede1 carboxyl-terminus promotes initiation and/or stabilization of an Hrr25/Ede1 endocytic initiation complex.

Hrr25 mammalian homologs, CK1δ and 1ε, are required for efficient initiation of clathrin-mediated endocytosis

If CK1 family members have a conserved role in endocytosis, they should also appear and function at sites of CME in human cells. We looked for colocalization of CK1δ with clathrin-coated structures (CCS) by transiently transfecting GFP-CK1δ (Zyss et al., 2011) and detected its association with 16.0% of the CCS (> 5000 CCS from 13 cells, Fig. S4A). Similarly, we detected by immunofluorescence endogenous CK1ε associated with 11.9% of AP2 punctae (> 3000 CCS from 10 cells, Fig. S4B). These incidences of co-detection are likely underestimates of co-localization because low signal-to-noise of the kinase made imaging challenging, and because we could not image both CK1 isoforms simultaneously. As a control we evaluated the chance of random colocalization by shifting the position of the same image and found 4.6% colocalization. Previously, clathrin was shown to appear at CCS in a short-lived (< 20 s) and a long-lived population (> 20 s), proposed to represent abortive and productive events, respectively (Grassart et al., 2014; Loerke et al., 2009). We therefore monitored GFP-CK1δ and clathrin light chain-RFP simultaneously for 4 min and found that GFP-CK1δ was detected at 15.9% of short-lived CCS and at 32.7% of long-lived CCS (Fig. 4B). Notably, CK1δ arrives during the first seconds in the appearance of both short-lived and long-lived CCS (as well as stable CCS) (Fig. 4A, C, D). The above results suggest that CK1δ functions in the early stages of the CME pathway.

Consistent with a previous genome-wide RNA interference screen (Collinet et al., 2010), we found that depletion of CK1δ (Fig. S4C) led to an approximately 60% and 20% reduction in EGF and transferrin uptake respectively (Fig. 4E and S4E). Loss of CK1ε or concomitant depletion of both kinases resulted in defects in EGF uptake of similar magnitude. Therefore, these kinases are necessary for and likely play redundant roles in efficient CME in mammalian cells. In addition, we observed that depletion of the casein kinases extended CCS lifetimes (Fig. 4F, H and Fig. S4F). Finally, we tested whether CCS initiation is affected when CK1δ and/or 1ε are depleted. When endocytic initiation was monitored over a 4 min window in siRNA-treated cells, a significant reduction in initiation events was observed (Fig. 4G, I). Depletion of CK1δ or 1ε reduced the CME initiation rate by 18.4% or 27.8%, respectively. Together, the above results provide evidence for functional conservation for CK1 family protein kinases in stabilizing the CCS during early stages of CME in mammalian cells and yeast.

Discussion

Earlier studies suggested that CME is regulated at multiple stages, including during initiation and stabilization of endocytic sites (Loerke et al., 2009). Recently there has been

much debate about the nature of the earliest events in the CME pathway and the identity of the key molecules involved (Cocucci et al., 2012; Henne et al., 2010; Umasankar et al., 2012). The studies presented here identified a conserved function for protein phosphorylation, mediated by CK1 family members, in the regulation of endocytic site initiation and stabilization. Our studies showed that Hrr25 is an early component of the endocytic machinery. Hrr25 recruitment to endocytic sites depends on Ede1 and on Hrr25's own kinase activity. Importantly, loss of Hrr25 or its kinase activity impairs endocytic site initiation, whereas Hrr25 overexpression increases the number of endocytic sites, indicating that Hrr25 activity is limiting for endocytic site initiation and/or stabilization.

Implication of a protein kinase in endocytic site initiation and stabilization by a combination of loss and gain of function manipulations, made identification of the relevant targets an important goal. Several endocytic proteins were phosphorylated by Hrr25 *in vitro*. An Hrr25 target that plays a key role in endocytic site initiation should be one that arrives at endocytic sites early and that is functionally important for early events. Ede1 meets both of these criteria. Evidence presented here showed that Ede1 is a cellular Hrr25 target. The combined loss of Ede1 and Hrr25 had a synergistic effect, suggesting that Hrr25 regulates endocytic site initiation and stabilization partly through Ede1 phosphorylation and partly through an Ede1-independent mechanism.

Since all of the yeast proteins studied here are highly conserved, it was expected that their functions would be conserved as well. Indeed, we showed that the human Hrr25 homologues CK1δ/ε, are present at CME sites and are required for efficient endocytic site initiation. Interestingly, we observed that CK1 depletion reduces the rate of transferrin internalization and the rate of CCS initiation by approximately 20%. Because multiple factors with apparently redundant functions participate the early stages of endocytosis (Brach et al., 2014), it was expected that CK1 depletion might have only a modest effect on CME. Because transferrin internalization is constitutive, our results suggest that the transferrin internalization defect is a direct consequence of the reduced CME initiation rate. Surprisingly, we observed that EGF internalization, which is induced, not constitutive, is strikingly more sensitive to CK1 depletion compared to transferrin (Fig. S4D). This observation may reflect an additional CK1 role in the regulatory mechanism for EGF internalization. Despite the higher complexity of CME in human cells compared to yeast, our data provide evidence that CK1 plays a universal role in endocytic site initiation and stabilization.

Experimental Procedures

Yeast strains and plasmids

The yeast strains and plasmids used in this study are listed in Supplemental Information. Cells were grown in YPD or selective medium at 25°C unless specified.

Mammalian cell culture and transfection

SK-MEL-2 hCLTA^{EN-1}, hDNM2^{EN-all} (clone Ti13) and SKMEL-2 hCLTA^{EN-1} (clone Ti96) cell lines were maintained as described in Doyon et al., 2011. Plasmid and siRNA

transfections were performed as described in Grassart et al., 2014. Lipofectamin2000 and LipofectaminRNAiMAX (Invitrogen) were used following the manufacturer's guidelines.

Live-cell imaging and image analysis

Live-cell imaging was performed as described in Supplemental Information. Patch lifetimes were analyzed using Imaris (Bitplane) software. For yeast cell images, individual cells were analyzed using the spot detector module with an estimated spot size 300 nm. For mammalian cell images, clathrin or dynamin spots were analyzed using Imaris as described in Doyon et al., 2011. To analyze Sla1-GFP patch numbers, a maximum intensity of the Z-projection for Sla1-GFP was analyzed using Icy software (de Chaumont et al., 2012) and confirmed by a visual inspection.

In vitro kinase assays and identification of Ede1 phosphorylation sites

Hrr25 and Hrr25(K38A) were purified as described in Supplemental Information. Both substrates and kinases were subjected to SDS-PAGE along with BSA standards and stained with GelCode Blue (Thermo Scientific). The protein concentrations were determined by measuring the intensities of the protein bands using an Odyssey Imaging System (LI-COR Biosciences). *In vitro* phosphorylation was performed as previously described (Peng and Weisman, 2008).

6x His-tagged Ede1C (900–1381aa) was overexpressed in *E. coli* and purified using Ni-NTA agarose beads (Qiagen) following manufacturer's manual. 400 μg of purified proteins was subjected to phosphorylation by Hrr25. Phosphorylated residues of Ede1C (900–1381 aa) were identified by tandem mass spectrometry analysis as previously described (Peng et al., 2011).

Supplementary Material

Refer to Web version on PubMed Central for supplementary material.

Acknowledgments

We thank Beverly Wendland, Linda Hicke, Patrick Lusk, Damien D'Amours, Susan Ferro-Novick, Santiago Di Pietro, and Fanni Gergely for sharing reagents. We especially thank Susheela Carroll for her help in the initial characterization of Hrr25 by fluorescence microscopy, and Alphée Michelot and Yidi Sun for providing purified endocytic proteins. This work is supported by NIH grants R01 GM50399 (D.G.D.), R01 GM47842 (G.B.) and P41 RR011823 (J.Y., III.).

References

Aguilar RC, Watson HA, Wendland B. The yeast Epsin Ent1 is recruited to membranes through multiple independent interactions. J Biol Chem. 2003; 278:10737–10743. [PubMed: 12529323]

Brach T, Godlee C, Moeller-Hansen I, Boeke D, Kaksonen M. The initiation of clathrin-mediated endocytosis is mechanistically highly flexible. Curr Biol. 2014; 24:548–554. [PubMed: 24530066]

Breitkreutz A, Choi H, Sharom JR, Boucher L, Neduva V, Larsen B, Lin ZY, Breitkreutz BJ, Stark C, Liu G, et al. A global protein kinase and phosphatase interaction network in yeast. Science. 2010; 328:1043–1046. [PubMed: 20489023]

Carroll SY, Stimpson HE, Weinberg J, Toret CP, Sun Y, Drubin DG. Analysis of yeast endocytic site formation and maturation through a regulatory transition point. Mol Biol Cell. 2011

Cocucci E, Aguet F, Boulant S, Kirchhausen T. The first five seconds in the life of a clathrin-coated pit. Cell. 2012; 150:495–507. [PubMed: 22863004]

Collinet C, Stoter M, Bradshaw CR, Samusik N, Rink JC, Kenski D, Habermann B, Buchholz F, Henschel R, Mueller MS, et al. Systems survey of endocytosis by multiparametric image analysis. Nature. 2010; 464:243–249. [PubMed: 20190736]

Cope MJ, Yang S, Shang C, Drubin DG. Novel protein kinases Ark1p and Prk1p associate with and regulate the cortical actin cytoskeleton in budding yeast. J Cell Biol. 1999; 144:1203–1218. [PubMed: 10087264]

Corbett KD, Harrison SC. Molecular architecture of the yeast monopolin complex. Cell Rep. 2012; 1:583–589. [PubMed: 22813733]

de Chaumont F, Dallongeville S, Chenouard N, Herve N, Pop S, Provoost T, Meas-Yedid V, Pankajakshan P, Lecomte T, Le Montagner Y, et al. Icy: an open bioimage informatics platform for extended reproducible research. Nat Methods. 2012; 9:690–696. [PubMed: 22743774]

Dephoure N, Gould KL, Gygi SP, Kellogg DR. Mapping and analysis of phosphorylation sites: a quick guide for cell biologists. Mol Biol Cell. 2013; 24:535–542. [PubMed: 23447708]

Fish KJ, Cegielska A, Getman ME, Landes GM, Virshup DM. Isolation and characterization of human casein kinase I epsilon (CKI), a novel member of the CKI gene family. J Biol Chem. 1995; 270:14875–14883. [PubMed: 7797465]

Gagny B, Wiederkehr A, Dumoulin P, Winsor B, Riezman H, Haguenauer-Tsapis R. A novel EH domain protein of Saccharomyces cerevisiae, Ede1p, involved in endocytosis. J Cell Sci. 2000; 113(Pt 18):3309–3319. [PubMed: 10954428]

Grassart A, Cheng AT, Hong SH, Zhang F, Zenzer N, Feng Y, Briner DM, Davis GD, Malkov D, Drubin DG. Actin and dynamin2 dynamics and interplay during clathrin-mediated endocytosis. J Cell Biol. 2014; 205:721–735. [PubMed: 24891602]

Henne WM, Boucrot E, Meinecke M, Evergren E, Vallis Y, Mittal R, McMahon HT. FCHo proteins are nucleators of clathrin-mediated endocytosis. Science. 2010; 328:1281–1284. [PubMed: 20448150]

Ho Y, Gruhler A, Heilbut A, Bader GD, Moore L, Adams SL, Millar A, Taylor P, Bennett K, Boutilier K, et al. Systematic identification of protein complexes in Saccharomyces cerevisiae by mass spectrometry. Nature. 2002; 415:180–183. [PubMed: 11805837]

Kafadar KA, Zhu H, Snyder M, Cyert MS. Negative regulation of calcineurin signaling by Hrr25p, a yeast homolog of casein kinase I. Genes Dev. 2003; 17:2698–2708. [PubMed: 14597664]

Kaksonen M, Toret CP, Drubin DG. A modular design for the clathrin- and actin-mediated endocytosis machinery. Cell. 2005; 123:305–320. [PubMed: 16239147]

Loerke D, Mettlen M, Yarar D, Jaqaman K, Jaqaman H, Danuser G, Schmid SL. Cargo and dynamin regulate clathrin-coated pit maturation. PLoS Biol. 2009; 7:e57. [PubMed: 19296720]

Lusk CP, Waller DD, Makhnevych T, Dienemann A, Whiteway M, Thomas DY, Wozniak RW. Nup53p is a target of two mitotic kinases, Cdk1p and Hrr25p. Traffic. 2007; 8:647–660. [PubMed: 17461799]

McIsaac RS, Silverman SJ, McClean MN, Gibney PA, Macinskas J, Hickman MJ, Petti AA, Botstein D. Fast-acting and nearly gratuitous induction of gene expression and protein depletion in Saccharomyces cerevisiae. Mol Biol Cell. 2011; 22:4447–4459. [PubMed: 21965290]

Mok J, Kim PM, Lam HY, Piccirillo S, Zhou X, Jeschke GR, Sheridan DL, Parker SA, Desai V, Jwa M, et al. Deciphering protein kinase specificity through large-scale analysis of yeast phosphorylation site motifs. Sci Signal. 2010; 3:ra12. [PubMed: 20159853]

Peng Y, Weisman LS. The cyclin-dependent kinase Cdk1 directly regulates vacuole inheritance. Dev Cell. 2008; 15:478–485. [PubMed: 18804442]

Peng Y, Wong CC, Nakajima Y, Tyers RG, Sarkeshik AS, Yates J 3rd, Drubin DG, Barnes G. Overlapping kinetochore targets of CK2 and Aurora B kinases in mitotic regulation. Mol Biol Cell. 2011; 22:2680–2689. [PubMed: 21633108]

Petronczki M, Matos J, Mori S, Gregan J, Bogdanova A, Schwickart M, Mechtler K, Shirahige K, Zachariae W, Nasmyth K. Monopolar attachment of sister kinetochores at meiosis I requires casein kinase 1. Cell. 2006; 126:1049–1064. [PubMed: 16990132]

Ptacek J, Devgan G, Michaud G, Zhu H, Zhu X, Fasolo J, Guo H, Jona G, Breitkreutz A, Sopko R, et al. Global analysis of protein phosphorylation in yeast. Nature. 2005; 438:679–684. [PubMed: 16319894]

Reider A, Barker SL, Mishra SK, Im YJ, Maldonado-Baez L, Hurley JH, Traub LM, Wendland B. Syp1 is a conserved endocytic adaptor that contains domains involved in cargo selection and membrane tubulation. Embo J. 2009; 28:3103–3116. [PubMed: 19713939]

Sadowski I, Breitkreutz BJ, Stark C, Su TC, Dahabieh M, Raithatha S, Bernhard W, Oughtred R, Dolinski K, Barreto K, et al. The PhosphoGRID Saccharomyces cerevisiae protein phosphorylation site database: version 2.0 update. Database (Oxford). 2013; 2013:bat026. [PubMed: 23674503]

Stark C, Su TC, Breitkreutz A, Lourenco P, Dahabieh M, Breitkreutz BJ, Tyers M, Sadowski I. PhosphoGRID: a database of experimentally verified in vivo protein phosphorylation sites from the budding yeast Saccharomyces cerevisiae. Database (Oxford). 2010; 2010:bap026. [PubMed: 20428315]

Stimpson HE, Toret CP, Cheng AT, Pauly BS, Drubin DG. Early-arriving Syp1p and Ede1p function in endocytic site placement and formation in budding yeast. Mol Biol Cell. 2009; 20:4640–4651. [PubMed: 19776351]

Taylor MJ, Perrais D, Merrifield CJ. A high precision survey of the molecular dynamics of mammalian clathrin-mediated endocytosis. PLoS Biol. 2011; 9:e1000604. [PubMed: 21445324]

Uezu A, Horiuchi A, Kanda K, Kikuchi N, Umeda K, Tsujita K, Suetsugu S, Araki N, Yamamoto H, Takenawa T, et al. SGIP1alpha is an endocytic protein that directly interacts with phospholipids and Eps15. J Biol Chem. 2007; 282:26481–26489. [PubMed: 17626015]

Umasankar PK, Sanker S, Thieman JR, Chakraborty S, Wendland B, Tsang M, Traub LM. Distinct and separable activities of the endocytic clathrin-coat components Fcho1/2 and AP-2 in developmental patterning. Nat Cell Biol. 2012; 14:488–501. [PubMed: 22484487]

Zeng G, Cai M. Regulation of the actin cytoskeleton organization in yeast by a novel serine/threonine kinase Prk1p. J Cell Biol. 1999; 144:71–82. [PubMed: 9885245]

Zyss D, Ebrahimi H, Gergely F. Casein kinase I delta controls centrosome positioning during T cell activation. J Cell Biol. 2011; 195:781–797. [PubMed: 22123863]

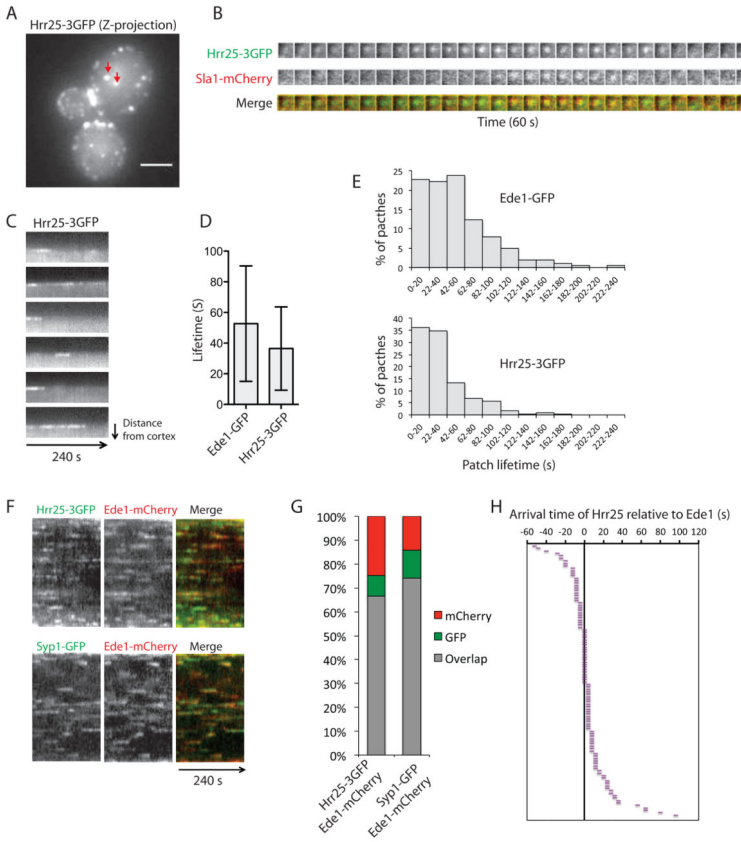

Figure 1. Yeast CK1 Hrr25 is an early-arriving endocytic protein

(A) Maximum Z-projection of Hrr25-3GFP. Red arrows point to SPBs. Scale bars, 2 μm. (B) Simultaneous two-color imaging of the medial focal planes of cells expressing Hrr25-3GFP and Sla1-mCherry. The time series shows an individual patch. Frame interval is 2 s. (C) Representative kymographs of Hrr25-3GFP illustrate variable lifetimes of Hrr25 on the plasma membrane. Images were acquired at 2 s intervals. (D) Average lifetimes of Ede1-GFP and Hrr25-3GFP ± standard deviations. Images were acquired at the medial focal plane of cells for 240 s with 2 s intervals. Ede1-GFP lifetime: n = 202 from 10 cells; Hrr25-3GFP lifetime: n = 248 from 10 cells. (E) Distribution of Ede1-GFP and Hrr25-3GFP lifetimes. The same data used in C are presented as percentages. (F) Simultaneous two-color imaging of medial focal planes of cells expressing Hrr25-3GFP or Syp1-GFP together with Ede1-mCherry at 2 s intervals with 2 s exposures. Representative kymographs are presented. (G) Percentages of overlapping patches during 4 min interval. (n = 373 from 12 cells expressing Hrr25-3GFP and Ede1-mCherry; n= 636 from 19 cells expressing Syp1-GFP and Ede1-mCherry). (H) Arrival times for Hrr25-3GFP relative to Ede1-mCherry are presented in a descending order (n = 110 from 23 cells). Each bar represents a single endocytic event. Negative or positive values represent Hrr25-3GFP arrival earlier or later than Ede1-mCherry, respectively.

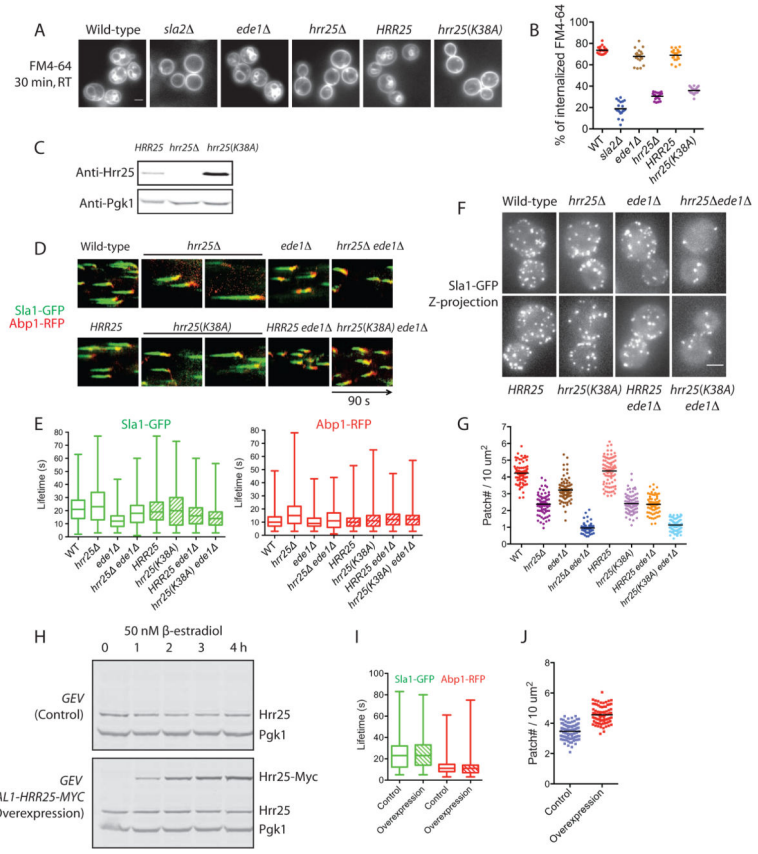

Figure 2. Loss of Hrr25 or its kinase activity results in formation of fewer endocytic sites, whereas Hrr25 overexpression increases the number of endocytic sites formed

(A) Wild-type and mutant cells were incubated with FM4-64 for 5 min and chased with fresh media for 30 min at RT. *HRR25* is the isogenic wild-type strain for *hrr25(K38A)*. (B) Percentages for internalized FM4-64 fluorescence intensity relative to whole cell FM4-64 fluorescence intensity are presented. 20 cells were scored for each strain and mean values are presented as black bars. (C) Cell extracts prepared from the indicated strains were analyzed by immunoblotting. (D) Simultaneous two-color imaging of medial focal planes of wild-type and mutant cells expressing Sla1-GFP and Abp1-RFP was performed continuously for 90 s. Representative kymographs are presented. (E) Lifetimes of Sla1-GFP and Abp1-RFP in wild-type and mutant cells. More than 300 Sla1-GFP or Abp1-RFP patches were tracked. Mean values and standard deviations (boxes) are presented. Whiskers indicate the minimum and maximum duration times. (F) Maximum Z-projection of Sla1-GFP patches in wild-type and mutant cells. (G) Quantification of Sla1-GFP patch numbers in wild-type and mutant cells. Sla1-GFP patches in unbudded or large-budded cells were scored using Icy software. The area used to calculate the patch density was the area of a sphere of the same radius as the circle on which all of the patches of the 3-D cell were projected for the maximum intensity. Averages (black bars) of more than 50 cells for each strain are presented. (H) Cells harboring either *GEV* (control) or *GEV* P_{GAL}*-HRR25-MYC* (Hrr25 overexpression) were grown to log phase, induced with 50 nM β-estradiol, and harvested at the indicated time points. Whole cell extracts were subjected to immunoblotting. Intensity of total Hrr25 (endogenous Hrr25 and overexpressed Hrr25-Myc)

at each time point was quantified, normalized to the intensity of Pgk1, and presented as ratios to the value for the 0 h time point. (I) Control cells and Hrr25 overexpression cells were induced with 50 nM of β-estradiol for 4 h and imaged for Sla1-GFP and Abp1-RFP lifetimes as described above in (E), n = 500. (J) Sla1-GFP patches were scored and calculations performed as described in (G). More than 80 cells for each strain were scored and mean values are presented as black bars. *** $P < 0.0001$. Scale bars, 2 μm.

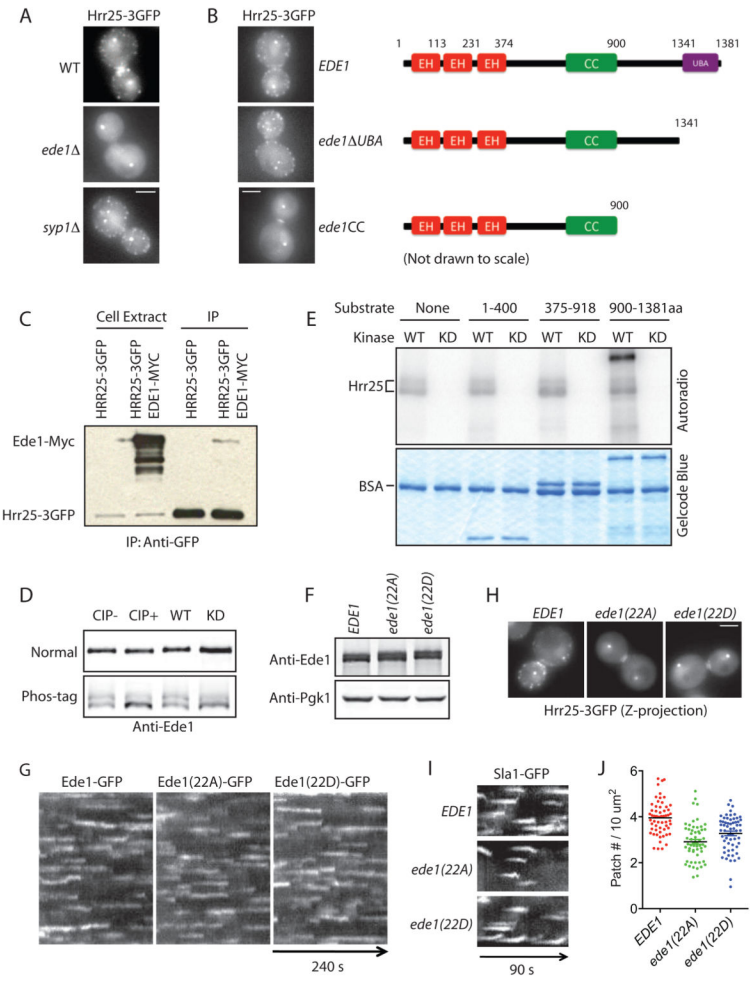

Figure 3. Ede1 phosphorylation by Hrr25 is required for Hrr25 recruitment to endocytic sites

(A) Maximum intensity projections of Hrr25-3GFP in wild-type, *ede1*Δ, and *syp1*Δ cells. (B) Maximum intensity projections of Hrr25-3GFP in the indicated *ede1* truncation mutants. (C) Hrr25-3GFP was immunoprecipitated using an anti-GFP antibody. Ede1-Myc was immunoblotted using an anti-Myc antibody. (D) Anti-Ede1 immunoblots. Whole cell extract from the truncation mutant *ede1*Δ*PPCC* expressing wild-type Hrr25 (left two lanes) was treated with or without Calf Intestinal Phosphatase (CIP) for 1 h at 30°C and then subjected to SDS-PAGE using normal acrylamide (top) or 10 μM Phos-tag acrylamide gels (bottom). Cells expressing wild-type (WT) or kinase-dead (KD) Hrr25 and Ede1ΔPPCC were grown to log phase and subjected to SDS-PAGE as above (right two lanes). (E) 400 ng of the indicated Ede1 fragments were incubated with 4 ng of Hrr25 or Hrr25(K38A) in the presence of [γ^{32}P]-ATP at RT for 30 min. Phosphorylation was analyzed by autoradiography following SDS-PAGE. (F) Whole cell extracts of *EDE1* and phospho-mutants were subjected immunoblot analysis using anti-Ede1 and anti-Pgk1 antibodies. (G) Cells expressing Ede1-GFP, Ede1(22A)-GFP and Ede1(22D)-GFP were imaged at medial focal planes at 2 s intervals. Representative kymographs are shown. (H) Maximum Z-projection of Hrr25-3GFP in *ede1* phospho-mutant cells. (I) Representative kymographs of Sla1-GFP of *ede1* phospho-mutant cells. (J) Sla1-GFP patch numbers for *ede1* phospho-

mutants. More than 50 cells for each strain were scored and mean values are presented as black bars. Scale bars, 2 μm.

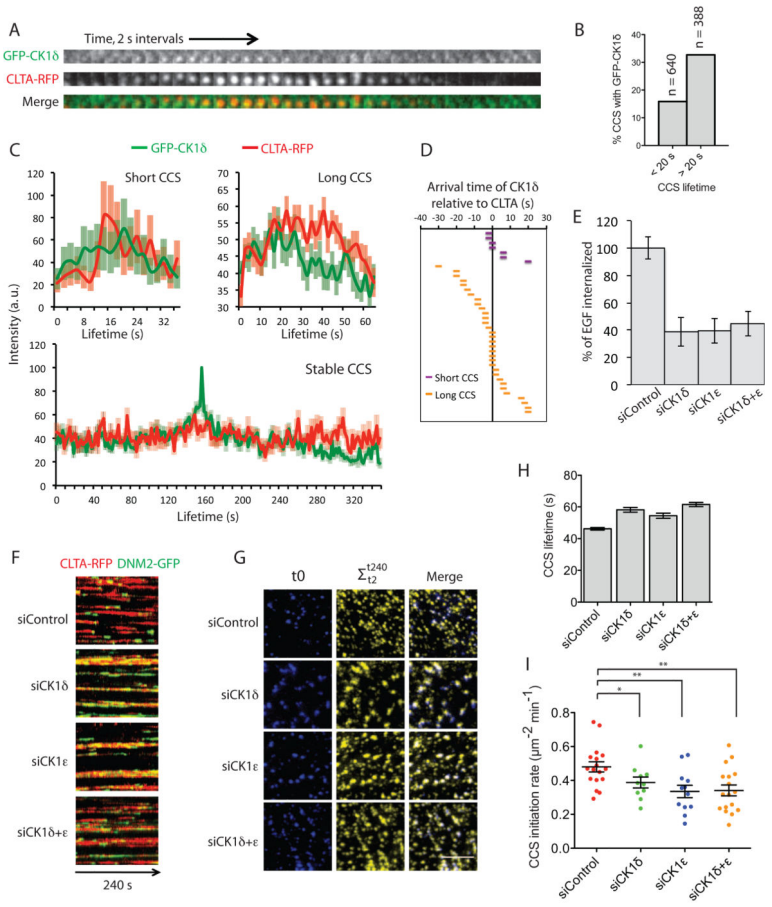

Figure 4. Hrr25 mammalian homologues CK1δ/ε are required for efficient *de novo* formation of clathrin-coated structures (CCS)

(A) GFP-CK1δ and CLTA-RFP were observed simultaneously by TIRF microscopy for 240 s. A representative montage is shown. (B) Percentages of CCS with GFP-CK1δ are presented (n = 1028 tracks from 3 cells). (C) Recruitment profile analysis for GFP-CK1δ and CLTA-RFP for clathrin tracks <20 s (short lived), 20–100 s (long lived), or > 240 s (stable) (n = 7, 32 and 16 respectively). (D) Arrival time of GFP-CK1δ relative to CCS initiation. Each bar represents a single endocytic event; purple bars represent short-lived CCS events (<20 s) and orange bars represent long-lived CCS events (>20 S). (E) Quantification of Alexa 647 coupled EGF uptake (2 ng/ml for 15 min) in SK-MEL-2 Ti96 cells knocked down for CK1δ and/or 1ε. The averages and standard errors of the mean (s.e.m.) from 3 independent experiments (n > 50 cells) are presented as percentages of control. (F) Representative kymographs of the lifetimes of CLTA-RFP and DNM2-GFP in SK-MEL-2 Ti13 cells knocked down for CK1δ and/or 1ε. (G) *De novo* CCS formation at the plasma membrane was observed by TIRF microscopy. CLTA-RFP image captured in the first frame (t_0) is shown in blue. Additional CCS formed during the next 240 s (t_2 to t_{240}) is shown in yellow. (H) Measurement of CLTA-RFP lifetimes in CK1δ and/or 1ε depleted cells (n > 2400 from 10 cells). Mean values and s.e.m. are presented. (I) Quantification of

CCS initiation rates of individual cells. Mean values and s.e.m are presented as bars in black ($n \geq 10$ cells). * $P < 0.05$; ** $P < 0.005$. Scale bars, 5 μm.